Petroleum Science 19 (2022) 1411–1419

Contents lists available at ScienceDirect

Petroleum Science

journal homepage: www.keaipublishing.com/en/journals/petroleum-science

Original Paper

A covering liquid method to intensify self-preservation effect for safety of methane hydrate storage and transportation

Jun Chen [a, b, *], Yao-Song Zeng [a], Xing-Yu Yu [a], Qing Yuan [b], Tao Wang [a], Bin Deng [a], Ke-Le Yan [c], Jian-Hong Jiang [a], Li-Ming Tao [a], Chang-Zhong Chen [a]

[a] Hunan Provincial Key Laboratory of Xiangnan Rare-Precious Metals Compounds and Applications, College of Chemistry and Environmental Science, Xiangnan University, Chenzhou, Hunan Province, 423000, China
[b] School of Chemistry and Chemical Engineering, Liaocheng University, Liaocheng, 252059, China
[c] SINOPEC Research Institute of Safety Engineering, 339 Songling Road, Qingdao, 266000, China

ARTICLE INFO

Article history:
Received 18 March 2021
Accepted 13 August 2021
Available online 12 November 2021

Edited by Xiu-Qiu Peng

Keywords:
Decomposition
Inhibition
Methane hydrate
Method
Self-preservation effect

ABSTRACT

In this work, experiments and comprehensive insights into the proposed covering liquid method to intensify self-preservation effect for methane (CH_4) storage are presented. The CH_4 hydrate decomposition percentage was 17.6% with the pressure of 0.61 MPa after 12 h at 266.0 K without a covering liquid, which can be reduced to 12.4%, 13.8%, 13.0%, and 8.3% with the pressure of 0.26 MPa, 0.33 MPa, 0.51 MPa, and 0.37 MPa by covering with tetrahydrofuran (THF), cyclopentane (CP), cyclohexane, and n-tetradecane, respectively. When the temperature for CH_4 hydrate decomposition was 274.2 K, covering with THF, CP, cyclohexane, and n-tetradecane failed to inhibit CH_4 hydrate decomposition. The results suggested that the covering liquid may form a new solid layer (a hydrate layer or other solidified layer) around the CH_4 hydrate, which inhibit CH_4 transfer below the freezing point of water. However, the new solid layer cannot resist the fast transfer of CH_4 from decomposed CH_4 hydrate above the freezing point of water. The same phenomenon was also observed in a sodium dodecyl sulfonate (SDS)-dry solution CH_4 hydrate formation system. Therefore, the covering method can only intensify the self-preservation effect below the freezing point of water, but cannot generate a self-preservation effect.

1. Introduction

Gas (such as methane) can be inserted into a water-constituted cage in the form of gas hydrate at elevated pressure and low temperature. Natural gas hydrate energy sources (Sun et al., 2019; Feng et al., 2017; Yang et al., 2019; Liu et al., 2018), plugs caused by gas hydrates (Ding et al., 2019; Park et al., 2017; Yan et al., 2014; Song et al., 2019; Xu et al., 2016 Saberi et al., 2020), and technologies derived from gas hydrates (Sa and Sum 2019; Shi et al., 2019; Wu et al., 2019; Zheng et al., 2019; Chen et al., 2019; Chazallon and Pirim, 2018; Rasoolzadeh et al., 2019; Xiao et al., 2018, 2019) were paid much attention for gas hydrate research in recent decades.

Methane (CH_4) storage and transportation by forming CH_4 hydrate is one of the technologies derived from the gas-concentrated properties of gas hydrate. One volume of CH_4 hydrate contained a 150–180 volume of CH_4 (Fan et al., 2014; Lim et al., 2014; Wang et al., 2014). The pressure for natural gas storage by forming natural gas hydrate was much lower than that of compressed natural gas (CNG) (20–30 MPa), which suggested that natural gas hydrate is a potential safe method for natural gas storage and transportation.

Both thermodynamic stable and unstable system of gas hydrate can be used for gas storage by hydrate-based technology. For thermodynamic stable system, gas was concentrated steadily as the form of the hydrate under the equilibrium conditions theoretically. Thermodynamic promoters, such as THF (Kumar et al., 2018), quaternary ammonium salt (Babu et al., 2014; Fan et al., 2016; Fukumoto et al., 2015), cyclohexane, and CP (Delroisse et al., 2018) can be added into hydrate formation systems to moderate the equilibrium conditions and accordingly reduce the pressure of gas

* Corresponding author. Hunan Provincial Key Laboratory of Xiangnan Rare-Precious Metals Compounds and Applications, College of Chemistry and Environmental Science, Xiangnan University, Chenzhou, Hunan Province, 423000, China.
E-mail address: chenjun4174@126.com (J. Chen).

https://doi.org/10.1016/j.petsci.2021.11.007

hydrate for gas storage. However, thermodynamic promoters also formed hydrates or semi-hydrates, which occupied hydrate cages and accordingly decreased the gas storage capacity. Therefore, as little as possible of the thermodynamic promoters was added in the consideration of gas storage capacity. From the thermodynamic unstable system, the self-preservation effect made it possible to be used in the gas storage and transportation at low pressures below 273.2 K (freezing point of water) (Stern et al., 2001a, b). When the temperature is below 273.2 K, gas hydrate decomposes slower than the common gas hydrate decomposition rate when the pressure and temperature are out of gas equilibrium conditions (Zhong et al., 2016; Xie et al., 2020, 2021). Zhang and Rogers (2008) found that the presence of Al tubes, Cu tubes, or solid copper can help the ultrastability of gas hydrates at ambient pressure and 268.2 K. Natural gas hydrate pellets can also be used for the long-term storage of natural gas hydrate at atmospheric pressure (Mimachi et al., 2015). From above two examples, additional methods are needed to enhance the self-preservation effect, and enhancement of self-preservation effect makes it possible for gas hydrate storage at lower and safer pressure, even 1 atm pressure. Therefore, intensification of self-preservation effect is still important and deserved further investigation. In addition, Takeya et al. (2001) investigated the self-preservation effect of CH_4 hydrate in situ by X-ray diffraction and proposed an ice-shielding model for the self-preservation effect. Although the accurate mechanism of self-preservation effect is still unknown (Stern et al., 2003), ice-shielding model was considered an acceptable mechanism to explain self-preservation effect (Falenty et al., 2014; Falenty and Kuhs, 2009).

From the inspiration of the ice-shielding model referenced above, a novel method was proposed to intensify self-preservation effect (Zeng et al., 2020). CH_4 is the main content in natural gas, and our previous publication has focused on CH_4 hydrate formation in sodium dodecyl sulfonate (SDS)-dry solution hydrate formation systems (Zeng et al., 2020). As a continuous work, the covering method focused on the hydrate samples formed with SDS solution by covering with THF, CP, cyclohexane, and n-tetradecane respectively in this work. In addition, comprehensive insight into the covering liquid method was also discussed in this work.

2. Experimental section

2.1. Experimental materials and apparatus

n-Tetradecane was purchased from Tianjin Weiyi Chemical Technology Co., Ltd. The details of CH_4, SDS, THF, CP, cyclohexane, and hydrophobic silica nanoparticles (HB630) can be found in a previous publication (Zeng et al., 2020). Four covering liquids of THF, CP, cyclohexane, and n-tetradecane have its own feature. THF, CP, and cyclohexane can form (THF + CH_4), (CP + CH_4), and (cyclohexane + CH_4) binary hydrate. THF is hydrophilic, while CP and cyclohexane are lipophilic. The solidifying point of cyclohexane is 279.7 K. Although n-tetradecane cannot form binary hydrate, the solidifying point of n-tetradecane is 279.2 K. Therefore, all above four chosen covering liquid may solidify as the form of hydrate or solid. HB630 were used to prepare SDS-dry solutions with SDS solution in the blender. The details of SDS-dry solution preparation can refer to previous work (Fan et al., 2014). An electronic balance with an accuracy of ±0.1 mg was used to weigh SDS. Double distilled water was prepared in our laboratory.

As shown in Fig. 1, the experimental apparatus is composed of two autoclaves, a temperature controlling system, and a data collection system. Each autoclave has an effective volume of 100 mL. The temperature can be adjusted by the temperature controlling system. The data of pressure and temperature can be automatically collected by the collected system. More details about the apparatus can be found in our previous publication (Zeng et al., 2020).

2.2. Experimental procedure

The experimental process included three experimental sections that were selection of the CH_4 hydrate formation system, CH_4 hydrate formation, and CH_4 hydrate decomposition.

2.2.1. Selection of the CH_4 hydrate formation system and CH_4 hydrate formed process

In this section, a CH_4 hydrate formation system was chosen to study the effect of the covering liquid method on self-preservation effect. Two autoclaves and relative connections were cleaned three times. Then, THF-SDS solution, CP-SDS solution, or cyclohexane-SDS solution was prepared by adding 12 mL of THF, CP, and cyclohexane into 30 mL of SDS solution with an SDS concentration of 500 ppm. After the solutions and autoclaves were prepared, the solution (SDS solution, THF-SDS solution, CP-SDS solution, or cyclohexane-SDS solution) was injected into autoclave 6 (as shown in Fig. 1). Then, autoclave 6, autoclave 7, and the connections were placed under vacuum to remove the air in both the gas and solution phases. The temperature of the glycol bath was set to the experimental value, and CH_4 was injected into autoclave 7. When the temperature reached the setting experimental value and then maintained for approximately 30 min, the CH_4 was injected from autoclave 7 into autoclave 6 until the pressure reached the desired value, and the CH_4 hydrate formation process started. After that, the whole process maintained for 5 h for each CH_4 hydrate formation system.

The SDS solution was finally chosen as the CH_4 hydrate formation system that was used for CH_4 hydrate decomposition in this work. Therefore, SDS solutions or SDS-dry solutions were used to form CH_4. The CH_4 hydrate can be considered finished when the pressure changes very little.

2.2.2. The covering liquid method

After CH_4 hydrate formed completely in the SDS solutions or SDS-dry solutions, CH_4 hydrate decomposition started. In order to prevent initial fast decomposition of CH_4 hydrate, initial temperature of CH_4 hydrate were 266.0 K. When the decomposition temperature was 266.0 K, the whole decomposition time was maintained for 12 h. When the decomposition temperature was 272.2 K and 274.2 K, the whole CH_4 hydrate formation system was maintained at 266.0 K for 1 h, and then set the temperature to the decomposition temperature. For the covering liquid, THF, CP, cyclohexane, and n-tetradecane were precooled to reduce heat exchange during covering process. Following processes were the details of the covering liquid method. For CH_4 hydrate decomposition at 266.0 K, valve 3 (as shown in Fig. 1) was open, to decrease CH_4 to 0.1 MPa within 1 min, and then, valve 3 was rapidly closed. The CH_4 hydrate decomposed under the situation without a covering liquid. The decomposition time was maintained for 12 h, and the pressure data were recorded. After 12 h, the experimental temperature was set to 293.2 K to make the CH_4 hydrate decomposed completely. If a covering liquid was used during the CH_4 hydrate decomposition process at 266.0 K, precooled liquid was injected into autoclave 6 (as shown in Fig. 1) by a hand pump after the CH_4 pressure in autoclave 6 was vented to 0.1 MPa. Then, all connections and valves were closed to allow CH_4 hydrate decomposition. The time for CH_4 hydrate decomposition processes was also maintained at 12 h. After 12 h, the experimental temperature was set to 293.2 K to make the CH_4 hydrate decomposes completely. The CH_4 hydrate decomposition percentage can be

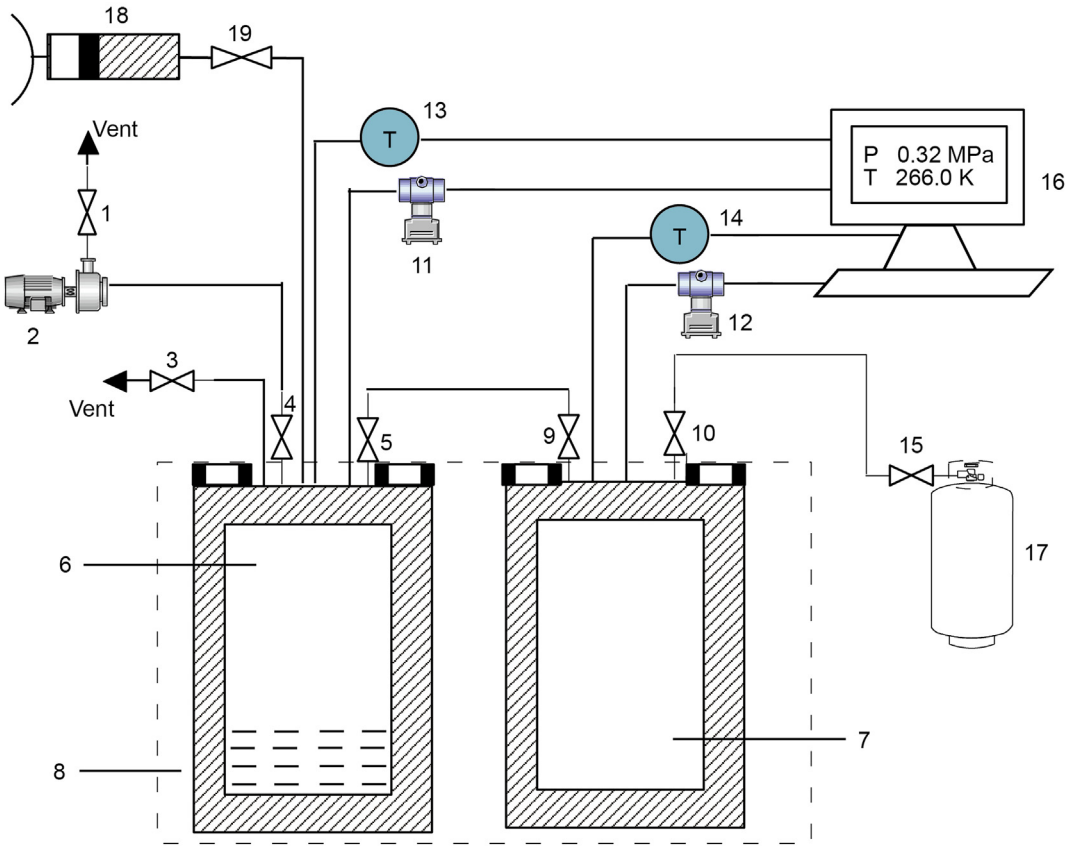

Fig. 1. Schematic diagram of the experimental apparatus. 1, Valve; 2, Vacuum pump; 3, 4, and 5, Valve; 6 and 7, Autoclave; 8, Glycol bath; 9 and 10, Valve; 11 and 12, Pressure transducer; 13 and 14, PT-100; 15 , Valve; 16, Computer; 17, Gas cylinder; 18, Hand pump; 19, Valve.

calculated by the following equation (Zeng et al., 2020):

$$y_{decomp.} = P_t / P_{final.} \times 100\% \quad (1)$$

Where $y_{decomp.}$ was the CH_4 hydrate decomposition percentage, $P_{final.}$ was the final pressure, and P_t was the pressure at time t in the process of hydrate decomposition. When CH_4 hydrate decomposed at 272.2 K and 274.2 K, the experimental temperature was first set and maintained at 266.0 K to inhibit fast CH_4 hydrate decomposition. For CH_4 hydrate decomposition without a covering liquid, the pressure was decreased to 0.1 MPa by valve 3 for CH_4 hydrate decomposition. Afterwards, the experimental temperature was maintained at 266.0 K for 1 h and then set to 272.0 K or 274.2 K to decompose CH_4 hydrate for another 12 h. Then, the experimental temperature was heated to 293.2 K to make CH_4 hydrate decomposes completely. For CH_4 hydrate decomposition with a covering liquid, the precooled covering liquid was injected into the autoclave by the hand pump after the pressure decreased to 0.1 MPa. After the temperature was maintained at 266.0 K for 1 h, the experimental temperature was set to 272.0 K or 274.2 K to decompose CH_4 hydrate for 12 h. After that, the experimental temperature was heated to 293.2 K to decompose CH_4 hydrate completely. The CH_4 hydrate decomposition percentage can also be calculated by equation (1).

3. Results and discussion

3.1. Selection of the CH_4 hydrates formation system

SDS is the kinetic promoter for CH_4 hydrate formation. THF, CP, cyclohexane are thermodynamic promoters for CH_4 hydrate formation. The kinetic promoter or (kinetic promoter + thermodynamic promoter) mixtures can accelerate gas hydrate process. Therefore, promoters of SDS, (THF + SDS), (CP + SDS), and (cyclohexane + SDS) were added to accelerate CH_4 hydrate formation at 274.2 K. The variation in pressure with time during the CH_4 hydrate formed process is shown in Fig. 2.

From Fig. 2, CH_4 pressure in gas phase decreased quickly during the first 30 min when CH_4 hydrate formed in SDS solution. The CH_4 pressure for CH_4 hydrate formation in SDS solution decreased to 2.94 MPa after 30 min, which was much lower than the pressures of 5.43 MPa, 5.95 MPa, and 5.83 MPa when CH_4 hydrate formed in the THF + SDS solution, CP + SDS solution, and cyclohexane + SDS solution systems after 30 min, respectively. No other guest molecule (CP, cyclohexane, or THF) occupied the hydrate cages, which resulted in the highest pressure reduction in 30 min when CH_4 hydrate formed in SDS solution. In addition, water-insoluble CP and cyclohexane can inhibit the transfer of CH_4, which results in a lower rate of CH_4 hydrate formation in the (CP + SDS solution) and (cyclohexane + SDS solution) systems than in the water-soluble THF-SDS solution. Fig. 2 also shows that the final pressure of CH_4 hydrates in SDS solution decreased to 2.80 MPa after 300 min of CH_4 hydrate formation, which was equal to the CH_4 hydrate formation pressure in bulk water (2.80 MPa at 274.2 K) calculated by the Chen-Guo hydrate model (Chen and Guo, 1998). However, when CH_4 hydrate formed in THF-SDS solution, CP-SDS solution, and cyclohexane-SDS solution, the final pressures after 300 min of CH_4 hydrate formation were 5.31 MPa, 5.64 MPa, and 5.50 MPa, respectively, which were much higher than the final pressure of CH_4 hydrate formation in SDS solution. The lowest final pressure

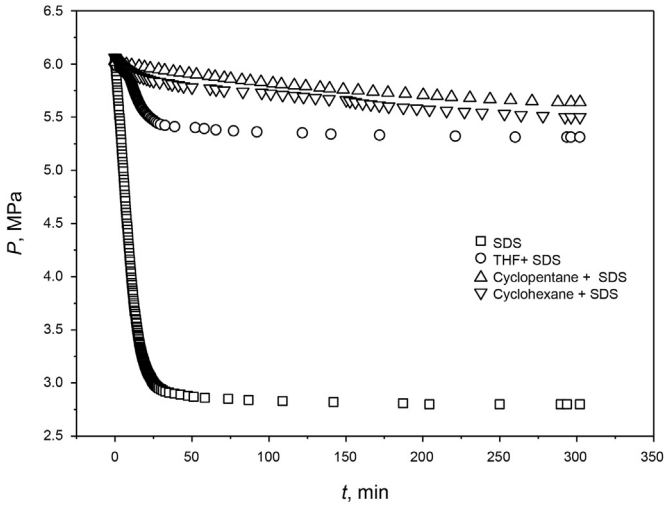

Fig. 2. Variation in pressure with time for CH_4 hydrates formation in different hydrate formation systems at 274.2 K.

suggested the highest amount of CH_4 consumption when CH_4 hydrate formed in SDS solution. CP, cyclohexane, and THF can occupy hydrate cages, which reduces CH_4 consumption for CH_4 hydrate formation in the (THF + SDS solution), (CP + SDS solution), and (cyclohexane + SDS solution) systems, respectively. In addition, gas-water ratio was not suitable for forming ideal CH_4 hydrate. Initial gas-water ratio for CH_4 hydrate formation in SDS solution was 168:1, which was lower than ideal gas-water ratio of 205:1 (1 volume of CH_4 hydrate contained 0.8 volume of water and 164 volume of CH_4). And the gas-liquid ratio for (THF + SDS solution), (CP + SDS solution), and (cyclohexane + SDS solution) decreased to 138:1, 139:1, and 140:1, respectively. Therefore, initial gas-water ratio also limited the formation was CH_4 hydrate. If the gas-water ratio was suitable, the CH_4 pressure would be close to the final pressure of CH_4 hydrate formation in SDS solution. In consideration of CH_4 consumption for CH_4 storage during methane hydrate formation process in this work, SDS solution was chosen as the CH_4 hydrate formation system for testing the covering method in the following experiments.

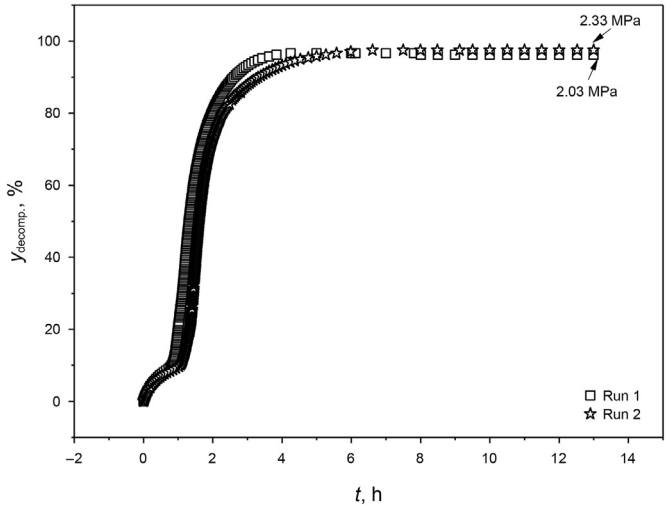

Fig. 3. Variation in CH_4 hydrate decomposition percentages with time for CH_4 hydrate decomposition in SDS-dry solution hydrate formation systems at 274.2 K.

3.2. The reliability of CH_4 hydrates decomposition

To test the reliability of CH_4 hydrate decomposition, two runs of CH_4 hydrate decomposition by covering with n-tetradecane were conducted in SDS-dry solution hydrate formation systems. The results are shown in Fig. 3.

From Fig. 3, the final pressure of CH_4 hydrate decomposition for Run 1 and Run 2 were 2.03 MPa and 2.33 MPa, respectively. And the final CH_4 hydrate decomposition percentages for Run 1 and Run 2 were 96.2% and 97.5%, respectively. The results suggested that the initial volume fraction of methane hydrate was different for methane hydrate formation process was a kinetic process. However, difference between the two runs was only 1.3%, which also suggested that the experiments can be repeated.

3.3. The results of the covering liquid method

3.3.1. Effect of covering liquid method on CH_4 hydrate decomposition at 266.0 K

CH_4 hydrate decomposition percentage with time was used to investigate the effect of the covering liquid (THF, CP, cyclohexane, and n-tetradecane) on CH_4 hydrate decomposition at 266.0 K. The reason to choose THF, CP, cyclohexane, and n-tetradecane as covering liquid is that all above four liquid may solidified when covering on the surface of CH_4 hydrate. THF, CP, and cyclohexane can form binary hydrate with CH_4 respectively (Sun et al., 2002; Lee et al., 2012). The equilibrium conditions of (CH_4+ THF) hydrate, (CH_4+ CP) hydrate, (CH_4+ cyclohexane) hydrate, and CH_4 hydrate were shown in Fig. 4. Cyclohexane and n-tetradecane can solidified at the experimental temperature during covering process. The variation in the CH_4 hydrates decomposition percentage with time is shown in Fig. 5.

From Fig. 5, CH_4 hydrate decomposed quickly, and the CH_4 hydrate decomposition percentage reached 11% in 1 h without covering with any liquid. The CH_4 hydrate decomposition process tended to slow down with continuously increasing time. The final CH_4 hydrate decomposition percentage was 17.6% after 12 h of decomposition with the pressure of 0.61 MPa, which suggested that a self-preservation phenomenon appeared at 266.0 K during the decomposed process.

In addition, the final percentage of 17.6% was less than final percentage of 25.5% for CH_4 hydrate decomposition in SDS-dry solution after 12 h of decomposition (Zeng et al., 2020). Water

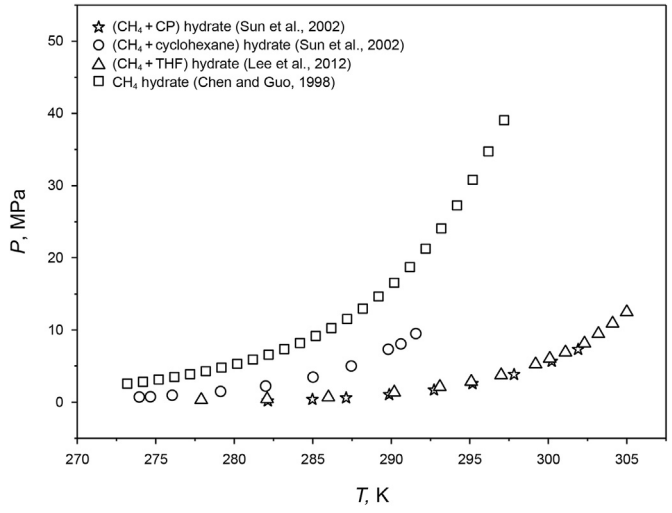

Fig. 4. Equilibrium conditions of CH_4 hydrate with/without addition of covering liquid.

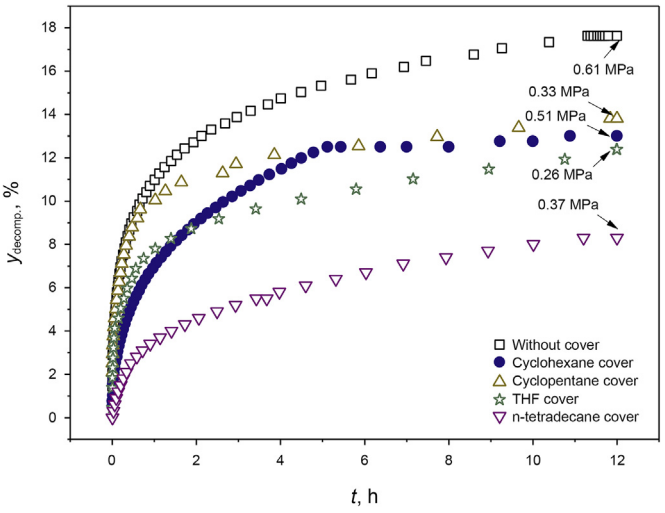

Fig. 5. Variation in CH_4 hydrate decomposition percentage with time by covering with different liquids at 266.0 K.

droplets in SDS-dry solution were smaller than water in SDS solution, which provided more surfaces for CH_4 hydrate formation. Therefore, there are more surfaces for CH_4 hydrate decomposition, which accordingly resulted in faster CH_4 hydrate decomposition in SDS-dry solution than in SDS solution. When the surface of CH_4 hydrate was covered by THF, CP, cyclohexane, and n-tetradecane, the same trends were observed respectively. CH_4 hydrate first decomposed quickly and then slowed down after a certain time. The final CH_4 hydrate decomposition percentages were 12.4%, 13.8%, 13.0%, and 8.3% with the pressures of 0.26 MPa, 0.33 MPa, 0.51 MPa, and 0.37 MPa by covering with THF, CP, cyclohexane, and n-tetradecane, respectively. The results suggested that covering with THF, CP, cyclohexane, and n-tetradecane effectively inhibited CH_4 hydrate decomposition, which accordingly enhanced the self-preservation effect. THF, CP, cyclohexane, and n-tetradecane have its own characteristics, which may affect the covering method to inhibit CH_4 hydrate decomposition. Covering with THF, CP, and cyclohexane can form (CH_4 + THF) hydrate, (CH_4 + CP) hydrate, and (CH_4 + cyclohexane) hydrate, respectively, which may provide a hydrate layer to inhibit CH_4 hydrate decomposition. CP, cyclohexane, and n-tetradecane are lipophilic, while THF is hydrophilic. Therefore, more THF than CP and cyclohexane may permeate between hydrates. In addition, the solidifying points of cyclohexane and n-tetradecane are 279.7 K and 279.0 K, respectively, and the cyclohexane and n-tetradecane coverings may solidify and adhere on CH_4 hydrate surface. From the discussion above, the hydrate layer and solidified layer formed a barrier that inhibited CH_4 transfer and accordingly inhibited CH_4 hydrate decomposition. In fact, the amount of covering liquid also affects CH_4 hydrate decomposition. 40 mL of THF was used to cover on the surface of CH_4 hydrate at 266.0 K. Fig. 6 showed variation of CH_4 hydrate decomposition percentage with time with 12 mL and 40 mL of covering THF, respectively.

From Figs. 6 and 40 mL of THF can effectively prevent CH_4 hydrate decomposition at 266.0 K CH_4 hydrate decomposition percentage was only 9.8% with the pressure of 0.25 MPa after 12 h when 40 mL of THF was covered on the CH_4 hydrate surface, which was smaller than 12.4% with the pressure of 0.26 MPa when 12 mL of THF was covered on the CH_4 hydrate surface. The results suggested more covering liquid was more effective to prevent CH_4 hydrate decomposition. More covering liquid increased the height on the CH_4 hydrate surface, which increased the resistance for CH_4 transfer, and according prevented CH_4 hydrate decomposition. If the covering liquid was sufficient, the covering method was similar to the immersion method proposed by Sharifi et al. (2018). In addition, the final CH_4 hydrate decomposition percentages in SDS solutions are also greater than the final CH_4 hydrate decomposition percentages in SDS-dry solutions (Zeng et al., 2020) by covering THF, CP, and cyclohexane, respectively.

3.3.2. *Effect of the covering liquid method on CH_4 hydrate decomposition at 274.2 K*

CH_4 hydrate decomposition with/without covering with THF, CP, cyclohexane, and n-tetradecane was also conducted at 274.2 K. The variation in the CH_4 hydrates decomposition percentage with time is shown in Fig. 7.

From Fig. 7, it can be seen that CH_4 hydrate decomposed quickly without a covering liquid at 274.2 K, and the CH_4 hydrate decomposition percentage increased to 70.5% after 3 h. The final decomposition percentage increased to 80.1% with the pressure of 2.64 MPa after 13 h of CH_4 hydrate decomposition, which suggested

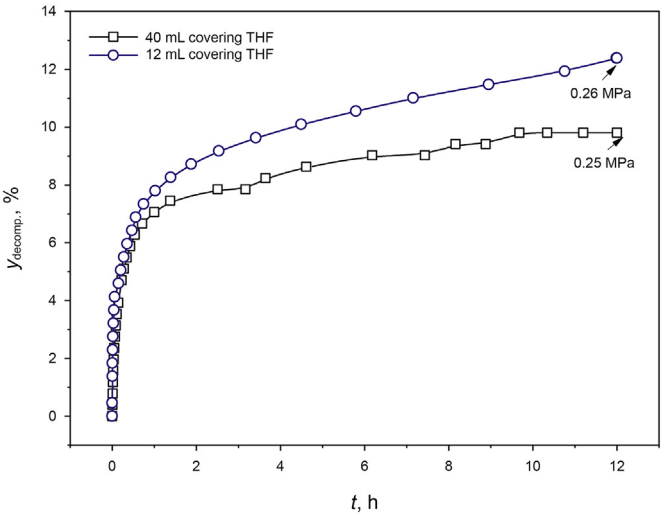

Fig. 6. Variation of CH_4 hydrate decomposition percentage with time at different covering THF quantity at 266.0 K.

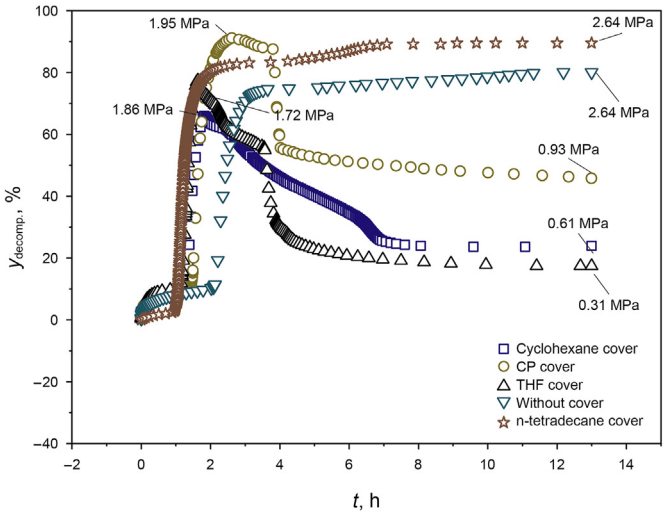

Fig. 7. Variation in CH_4 hydrate decomposition percentage with time at 274.2 K with different covering liquids.

that self-preservation effect vanished at 274.2 K without a covering liquid. There was no self-preservation effect observed above 273.2 K for gas hydrate decomposition previously. Therefore, CH_4 hydrate decomposed quickly when the conditions were out of equilibrium conditions. When CP, cyclohexane, and THF was used to cover the surface of CH_4 hydrate, CH_4 hydrate also decomposed quickly, and the maximum decomposition percentages reached 91.1%, 66.0%, and 77.4% with the pressure of 1.95 MPa, 1.86 MPa, and 1.72 MPa after 2.6 h, 1.8 h, and 1.6 h, respectively. The quickly increasing CH_4 hydrate decomposition percentage also suggested that the self-preservation effect also disappeared at the temperature of 274.2 K, even by covering CP, cyclohexane, and THF. Afterwards, the CH_4 hydrate decomposition percentage started to decrease, and the final decomposition percentage achieved by covering with CP, cyclohexane, and THF decreased to 45.8%, 23.9%, and 17.4% with the pressure of 0.93 MPa, 0.61 MPa, and 0.31 MPa after 13 h of CH_4 hydrate decomposition, respectively. Initial quick increase of CH_4 hydrate decomposition percentage from 1 h to 3 h by covering CP, cyclohexane, and THF suggested that the covering liquid method failed to inhibit quick decomposition of CH_4 hydrate and simultaneously failed to prevent fast transfer of CH_4. Combined the results with section 3.3.1, it revealed that covering with THF, CP, cyclohexane can only enhance self-preservation but cannot generate self-preservation. In addition, CH_4 hydrate decomposition percentage decreased with continuous increasing of time by covering THF, CP, and cyclohexane, respectively. The decrease in decomposition percentage suggested that binary hydrates of (CH_4+CP) hydrate, (CH_4 + cyclohexane) hydrate, and (CH_4+THF) hydrate formed. The reason for the formation of binary hydrate ascribed to that the conditions at the time of CH_4 hydrate decomposition percentage decreased was higher than the conditions for binary hydrate formation conditions. However, the decomposition percentage started to decrease at different times by covering with different liquids. The equilibrium pressures for (CH_4+CP) hydrate, (CH_4+cyclohexane) hydrate and (CH_4 + THF) hydrate at 282.15 K, 282.02 K, and 282.1 K were 0.165 MPa, 2.212 MPa, and 0.44 MPa respectively as shown in Fig. 4 (Sun et al., 2002; Lee et al., 2012). The time for forming (CH_4+CP) hydrate should be shorter than that for forming (CH_4+THF) hydrate, and the longest time should be for the formation of (CH_4+cyclohexane) hydrate. However, hydrate formation was stochastic because the induction time for hydrate formation was stochastic (Chen et al., 2019), which resulted in the stochastic formation times of (CH_4+CP) hydrate, (CH_4+THF) hydrate, and (CH_4+cyclohexane) hydrate. Therefore, the time for the reduction in the CH_4 hydrate decomposition percentage was also stochastic, as shown in Fig. 7. To cover with n-tetradecane at 274.2 K, CH_4 hydrate decomposed quickly after the temperature increased, and the CH_4 hydrate decomposition percentage reached 80% in the first 2 h of decomposition. The quick decomposition of CH_4 hydrate also suggested the disappearance of the self-preservation effect at 274.2 K, and covering n-tetradecane was ineffective to inhibit CH_4 hydrate decomposition at 274.2 K. After 13 h, the final CH_4 hydrate decomposition percentage increased to 89.5% with the pressure of 2.64 MPa. Although n-tetradecane solidified at 274.2 K, covering with n-tetradecane cannot inhibit fast CH_4 transfer during CH_4 hydrate decomposition. From the results of covering with THF, CP, cyclohexane, and n-tetradecane, all covering liquids failed to inhibit CH_4 hydrate decomposition at 274.2 K. THF, CP and cyclohexane can maintain relatively low CH_4 hydrate decomposition percentages at later stages by forming binary hydrates, while n-tetradecane cannot maintain relatively low CH_4 hydrate decomposition percentages, even though n-tetradecane cannot solidify at 274.2 K.

3.3.3. CH_4 hydrate decomposition from the SDS-dry solution hydrate formation system by covering with n-tetradecane

SDS-dry solution was produced to increase CH_4 hydrate formation by changing the water to many water droplets with small diameters (Fan et al., 2014; Wang et al., 2008). Previous publications have studied covering with THF, CP, and cyclohexane to inhibit CH_4 hydrate formation in SDS-dry solution hydrate formation systems. In this section, CH_4 hydrate decomposition by covering with n-tetradecane is conducted at different temperatures. The results are shown in Fig. 8. For convenient comparison, CH_4 hydrate decomposed without covering n-tetradecane was also shown in Fig. 8.

From Fig. 8, when the CH_4 hydrate decomposition temperature was 266.0 K without covering with n-tetradecane, the CH_4 hydrate decomposition percentage was 11.7% after 1 h of decomposition, and the CH_4 hydrate decomposition percentage reached 25.5% with the pressure of 0.61 MPa after 12 h of decomposition. When n-tetradecane was used, the CH_4 hydrate decomposition percentage decreased to 5.8% after 1 h of decomposition. The results indicated that covering with n-tetradecane can effectively inhibit initial CH_4 hydrate decomposition. Interestingly, the CH_4 hydrate decomposition percentage reached 25.0% after 12 h of decomposition with the pressure of 0.48 MPa, which was similar to 25.5% after 12 h of decomposition without covering with n-tetradecane at 266.0 K. The results suggested that covering with n-tetradecane may have little effect on CH_4 hydrate decomposition in SDS-dry solution hydrate formation systems. When the CH_4 hydrate decomposition temperature increased to 272.2 K, the CH_4 hydrate decomposition percentage was 48.5% after 12 h of decomposition, and the final CH_4 hydrate decomposition percentage increased to 49.4% with the pressure of 1.14 MPa by covering with n-tetradecane after 13 h of decomposition. The results demonstrated that the self-preservation effect was weakening at 272.2 K than that at 266.0 K. The CH_4 hydrate decomposition percentage without covering with n-tetradecane at 272.2 K reached 71.1% with the pressure of 1.33 MPa after 12 h of decomposition, as reported in our previous publication (Zeng et al., 2020). The results also suggested that covering with n-tetradecane can effectively inhibit CH_4 hydrate decomposition at 272.2 K and accordingly intensify the self-

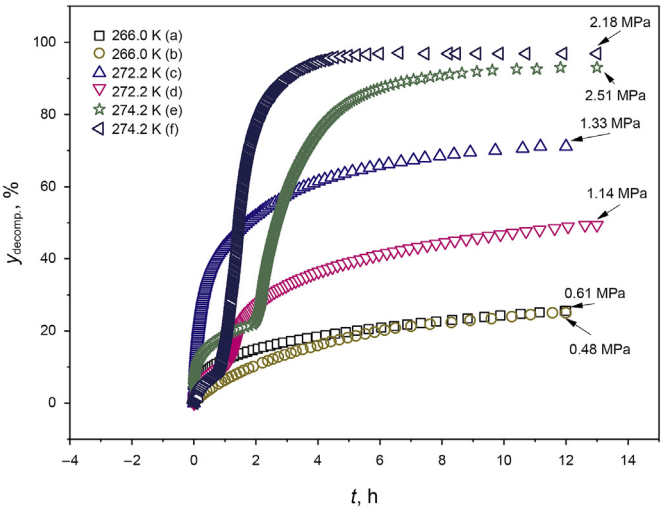

Fig. 8. Variation in CH4 hydrate decomposition percentages with time for CH4 hydrate decomposition by covering n-tetradecane in SDS-dry solution hydrate formation systems at different temperatures. (a), (c), and (e) was no covering process during methane hydrate decomposition at 266.0 K, 272.2 K, and 274.2 K, respectively (Zeng et al., 2020); (b), (d), and (f) was CH4 hydrate decomposition by covering n-tetradecane at 266.0 K, 272.2 K, and 274.2 K, respectively.

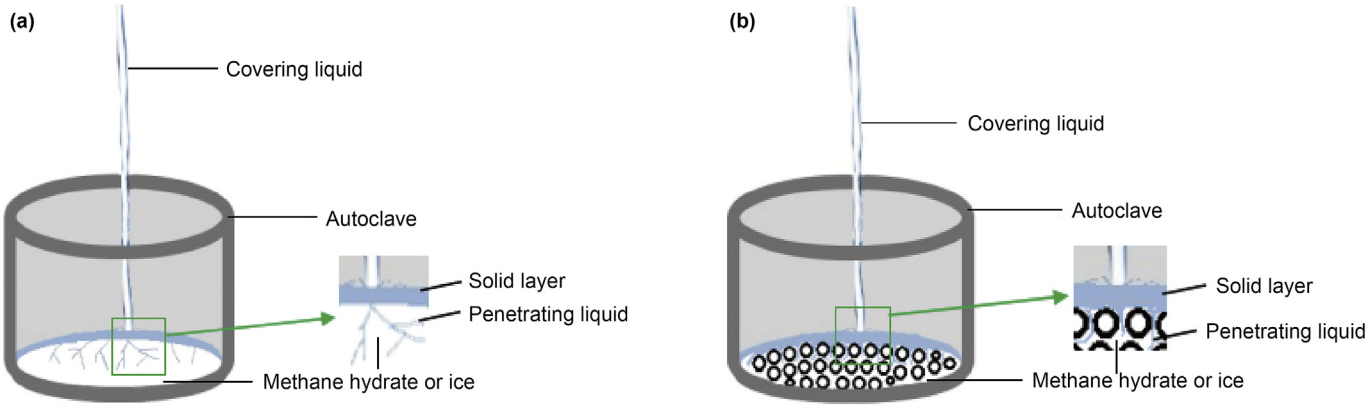

Fig. 9. Schematic diagram of the covering liquid method to inhibit CH_4 hydrate decomposition. (a) CH_4 hydrate formation in SDS solution; (b) CH_4 hydrate formation in SDS-dry solution.

preservation effect. When the temperature increased to 274.2 K, the CH_4 hydrate decomposition percentage reached 76.5% after 2 h, and the final CH_4 hydrate decomposition percentage reached 96.8% with the pressure of 2.18 MPa after 13 h of decomposition. CH_4 hydrate decomposed at 274.2 K suggested that the self-preservation effect vanished when the CH_4 hydrate decomposition temperature was above 273.2 K (freezing point of water), even when the covering n-tetradecane method was used. CH_4 hydrate decomposed from the SDS-dry solution hydrate formation system by covering with CP, cyclohexane, and THF, as can be found in our previous publication (Zeng et al., 2020). The results of covering with CP, cyclohexane, THF, and n-tetradecane in the SDS-dry solution hydrate formation system also show that the covering liquid can only enhance the self-preservation effect but cannot generate a self-preservation effect. In addition, hydrate particle size may affect the covering method to inhibit CH_4 hydrate decomposition. From the results of section 3.3.1, section 3.3.2, section 3.3.3, and our previous publication (Zeng et al., 2020), the covering liquid method was more effective in the SDS solution hydrate formation system (larger hydrate particles) than in the SDS-dry solution hydrate (smaller hydrate particles) formation systems.

3.4. Insights into the covering liquid method to inhibit CH_4 hydrate decomposition

From the results and discussion in section 3.3 and a previous publication (Zeng et al., 2020), a comprehensive schematic diagram of CH_4 hydrate decomposition by a covering liquid is shown in Fig. 9.

Combining section 3.2 and our previous publication (Zeng et al., 2020) with Fig. 9, the covering liquid method can only enhance the self-preservation effect below the freezing point of water, which means that the covering liquid method proposed in this work may not generate a self-preservation effect. When the covering liquid method was used for CH_4 hydrate decomposition from the SDS solution CH_4 hydrate formation system below the freezing point of water, as shown in Fig. 9(a), a solid layer (binary hydrate or solidified liquid) formed on top of the CH_4 hydrate to inhibit CH_4 transfer and accordingly intensify the self-preservation effect. In addition, some liquid may penetrate into CH_4 hydrates, which may affect the efficiency of the covering method. The amount of penetrating liquid was affected by the density of the covering liquid, the hydrophilicity of the covering liquid, and other possible factors.

For the SDS-dry solution CH_4 hydrate formation system, as shown in Fig. 9(b), the covering method can also only enhance the self-preservation effect below the freezing point of water but cannot generate a self-preservation effect. Except for the factors of the solid layer (binary hydrate or solidified liquid), the density of the covering liquid, equilibrium conditions of binary hydrate, and the hydrophilicity of the covering liquid can affect the covering method. The hydrate particle size may also affect the penetrating liquid and accordingly affect the efficiency of the covering method.

When the temperature was above the freezing point of water, the self-preservation effect vanished for CH_4 hydrate decomposition in both SDS solution and SDS-dry solution. The solid layer formed from the covering liquid may not inhibit so much CH_4 gas obtained from CH_4 hydrate decomposition and finally fails to inhibit CH_4 hydrate decomposition. The possible reason that the covering liquid method failed to inhibit CH_4 hydrate decomposition was the fast decomposition of CH_4 hydrate, which obtained a large amount of CH_4, and the formed solid layer could not support enough force to resist the pressure from CH_4. Therefore, covering with CP, cyclohexane, THF, and n-tetradecane can only enhance the self-preservation effect but cannot generate a self-preservation effect.

4. Conclusions

CH_4 hydrate decomposition by covering with THF, CP, cyclohexane, and n-tetradecane was conducted at temperatures both below the freezing point of water and above the freezing point of water. The following conclusions and insights were obtained.

(1) Covering with THF, CP, cyclohexane, and n-tetradecane can inhibit CH_4 hydrate decomposition and accordingly enhance the self-preservation effect for CH_4 hydrate formation in the SDS solution at 266.0 K. Covering with THF, CP, cyclohexane, and n-tetradecane can decrease the CH_4 hydrate decomposition percentage from 17.6% with the pressure of 0.61 MPa without covering with any liquid to 12.4%, 13.8%, 13.0%, and 8.3% with the pressures of 0.26 MPa, 0.33 MPa, 0.51 MPa, and 0.37 MPa by covering with THF, CP, cyclohexane, and n-tetradecane, respectively.
(2) Covering with THF, CP, cyclohexane, and n-tetradecane cannot inhibit CH_4 hydrate decomposition at 274.2 K, which suggested that the covering liquid method may not generate a self-preservation effect. However, binary hydrate formation can decrease the CH_4 hydrate decomposition percentage by covering with THF, CP, and cyclohexane at later stages.
(3) CH_4 hydrate particles may affect the covering method to inhibit CH_4 hydrate decomposition. Smaller hydrate particles

tend to increase CH_4 hydrate decomposition by using the covering liquid method.

(4) The hydrophilicity, density, solidifying point, and equilibrium conditions of binary hydrate may affect the covering method to inhibit CH_4 hydrate decomposition.

(5) Only solid layer cannot inhibit fast decomposition of CH_4 hydrate, which results in the failure of covering with THF, CP, cyclohexane, and n-tetradecane to inhibit CH_4 hydrate decomposition at 274.2 K.

Acknowledgments

This work is supported by the Hunan Provincial Natural Science Foundation of China (Nos. 2020JJ3030, 2019JJ50567), the National Natural Science Foundation of China (Nos. 21506065, 21978126, and 51904330), the Projects of Scientific Research Fund of Hunan Provincial Education Department (No. 17A199), and the Scientific Research Foundation of Xiangnan University for High-Level Talents.

References

Babu, P., Yao, M.H., Datta, S., Kumar, R., Linga, P., 2014. Thermodynamic and kinetic verification of tetra-n-butyl ammonium nitrate ($TBANO_3$) as a promoter for the clathrate process applicable to precombustion carbon dioxide capture. Environ. Sci. Technol. 48, 3550–3558. https://doi.org/10.1021/es4044819.

Chazallon, B., Pirim, C., 2018. Selectivity and CO_2 capture efficiency in CO_2-N_2 clathrate hydrates investigated by in-situ Raman spectroscopy. Chem. Eng. J. 342, 171–183. https://doi.org/10.1016/j.cej.2018.01.116.

Chen, G.J., Guo, T.M., 1998. A new approach to gas hydrate modeling. Chem. Eng. J. 71, 145–151. https://doi.org/10.1016/S1385-8947(98)00126-0.

Chen, J., Chen, G.J., Yuan, Q., Deng, B., Tao, L.M., Li, C.H., Xiao, S.X., Jiang, J.H., Li, X., Li, J.Y., 2019a. Insights into induction time and agglomeration of methane hydrate formation in diesel oil dominated dispersed systems. Energy 170, 604–610. https://doi.org/10.1016/j.energy.2018.12.138.

Chen, J., Wang, T., Zeng, Z., Jiang, J.H., Deng, B., Chen, C.Z., Li, J.Y., Li, C.H., Tao, L.M., Li, X., Xiao, S.X., 2019b. Oleic acid potassium soap: a new potential kinetic promoter for methane hydrate formation. Chem. Eng. J. 36, 349–355. https://doi.org/10.1016/j.cej.2019.01.148.

Delroisse, H., Plantier, F., Marlin, L., Dicharry, C., Frouté, L., AndréR, T.P., 2018. Determination of thermophysical properties of cyclopentane hydrate using a stirred calorimetric cell. J. Chem. Therm. 125, 136–141. https://doi.org/10.1016/j.jct.2018.05.023.

Ding, L., Shi, B.H., Liu, Y., Song, S.F., Wang, W., Wu, H.H., Gong, J., 2019. Rheology of natural gas hydrate slurry: effect of hydrate agglomeration and deposition. Fuel 239, 126–137. https://doi.org/10.1016/j.fuel.2018.10.110.

Falenty, A., Kuhs, W.F., Glockzin, M., Rehder, G., 2014. Selfpreservation of CH_4 hydrates for gas transport technology: pressure-temperature dependence and ice microstructures. Energy Fuels 28, 6275–6283. https://doi.org/10.1021/ef501409g.

Falenty, A., Kuhs, W.F., 2009. Self-preservation of CO_2 gas hydrates surface microstructure and ice perfection. J. Phys. Chem. B 113, 15975–15988. https://doi.org/10.1021/jp906859a.

Fan, S.S., Long, X.J., Lang, X.M., Wang, Y.H., Chen, J., 2016. CO_2 capture from CH_4/CO_2 mixture gas with tetranbutylammonium bromide semi-clathrate hydrate through a pressure recovery method. Energy Fuels 30, 8529–8534. https://doi.org/10.1021/acs.energyfuels.6b01615.

Fan, S.S., Yang, L., Wang, Y.H., Lang, X.M., Wen, Y.G., Lou, X., 2014. Rapid and high capacity methane storage in clathrate hydrates using surfactant dry solution. Chem. Eng. Sci. 106, 53–59. https://doi.org/10.1016/j.ces.2013.11.032.

Fukumoto, A., Silva, L.P.S., Paricaud, P., Dalmazzone, D., Fürst, W., 2015. Modeling of the dissociation conditions of H_2 + CO_2 semiclathrate hydrate formed with TBAB, TBAC, TBAF, TBPB, and $TBNO_3$ salts. Application to CO_2 capture from syngas. Int. J. Hydrogen Energy 40, 9254–9266. https://doi.org/10.1016/j.ijhydene.2015.05.139.

Feng, J.C., Wang, Y., Li, X.S., 2017. Entropy generation analysis of hydrate dissociation by depressurization with horizontal well in different scales of hydrate reservoirs. Energy 125, 62–71. https://doi.org/10.1016/j.energy.2017.02.104.

Kumar, A., Vedula, S.S., Kumar, R., Linga, P., 2018. Hydrate phase equilibrium data of mixed methane-tetrahydrofuran hydrates in saline water. J. Chem. Therm. 117, 2–8. https://doi.org/10.1016/j.jct.2017.05.014.

Lee, Y.J., Kawamura, T., Yamamoto, Y., Yoon, J.H., 2012. Phase equilibrium studies of tetrahydrofuran (THF) + CH_4, THF + CO_2, CH_4 + CO_2, and THF + CO_2 + CH_4 hydrates. J. Chem. Eng. Data 57, 3543–3548. https://doi.org/10.1021/je300850q.

Lim, S.H., Riffat, S.B., Park, S.S., Oh, S.J., Chun, W., Kim, N.J., 2014. Enhancement of methane hydrate formation using a mixture of tetrahydrofuran and oxidized multi-wallcarbon nanotubes. Int. J. Energy Res. 38, 374–379. https://doi.org/10.1002/er.3051.

Liu, H., Guo, P., Zhan, S.Y., Ma, P.J., Wei, N., Zhao, J.Z., Qiu, Y.L., 2018. Experimental investigation into formation/dissociation characteristics of methane hydrate in consolidated sediments with resistance measurement. Fuel 234, 985–995. https://doi.org/10.1016/j.fuel.2018.07.101.

Mimachi, H., Takahashi, M., Takeya, S., Gotoh, Y., Yoneyama, A., Hyodo, K., Takeda, T., Murayama, T., 2015. Effect of long-term storage and thermal history on the gas content of natural gas hydrate pellets under ambient pressure. Energy Fuels 29, 4827–4834. https://doi.org/10.1021/acs.energyfuels.5b00832.

Park, J., Silveira, K.C.D., Qi, S., Wood, C.D., Seo, Y., 2017. Performance of poly (N-isopropylacrylamide)-based kinetic hydrate inhibitors for nucleation and growth of natural gas hydrates. Energy Fuels 31, 2697–2704. https://doi.org/10.1021/acs.energyfuels.6b03369.

Rasoolzadeh, A., Javanmardi, J., Mohammadi, A.H., 2019. An experimental study of the synergistic efects of BMIM-BF4, BMIM-DCA and TEACl aqueous solutions on methane hydrate formation. Petrol. Sci. 16, 409–416. https://doi.org/10.1007/s12182-019-0302-1.

Sa, J.H., 2019. Sum AK Promoting gas hydrate formation with ice-nucleating additives for hydrate-based applications. Appl. Energy 251, 113352. https://doi.org/10.1016/j.apenergy.2019.113352.

Saberi, A., Alamdari, A., Rasoolzadeh, A., Mohammadi, A.H., 2020. Insights into kinetic inhibition efects of MEG, PVP, and L-tyrosine aqueous solutions on natural gas hydrate formation. Petrol. Sci. https://doi.org/10.1007/s12182-020-00515-0 doi.org/.

Sharifi, H., Yoneyama, A., Takeya, S., Ripmeester, J., Englezos, P., 2018. Superheating clathrate hydrates for anomalous preservation. J. Phys. Chem. C 122, 17019–17023. https://doi.org/10.1021/acs.jpcc.8b02930.

Shi, L.L., Ding, J.X., Liang, D.Q., 2019. Enhanced CH_4 storage in hydrates with the presence of sucrose stearate. Energy 180, 978–988. https://doi.org/10.1016/j.energy.2019.05.151.

Stern, L.A., Circone, S., Kirby, S.H., Durham, W.B., 2001a. Anomalous preservation of pure methane hydrate at 1 atm. J. Phys. Chem. B 105, 1756–1762. https://doi.org/10.1021/jp003061s.

Stern, L.A., Circone, S., Kirby, S.H., Durham, W.B., 2001b. Preservation of methane hydrate at 1 atm. Energy Fuels 15, 499–501. https://doi.org/10.1021/ef000277k.

Stern, L.A., Circone, S., Kirby, S.H., Durham, W.B., 2003. Temperature, pressure, and compositional effects on anomalous or "self" preservation of gas hydrates. Can. J. Phys. 81, 271–283. https://doi.org/10.1139/p03-018.

Song, G.C., Li, Y.X., Wang, W.C., Jiang, K., Shi, Z.Z., Yao, S.P., 2019. Hydrate agglomeration modeling and pipeline hydrate slurry flow behavior simulation. Chin. J. Chem. Eng. 27, 32–43. https://doi.org/10.1016/j.cjche.2018.04.004.

Sun, Z.F., Li, N., Jia, S., Cui, J.L., Yuan, Q., Sun, C.Y., Chen, G.J., 2019. A novel method to enhance methane hydrate exploitation efficiency via forming impermeable overlying CO2 hydrate cap. Appl. Energy 240, 842–850. https://doi.org/10.1016/j.apenergy.2019.02.022.

Sun, Z.G., Fan, S.S., Guo, K.H., Shi, L., Guo, Y.K., Wang, R.Z., 2002. Gas hydrate phase equilibrium data of cyclohexane and cyclopentane. J. Chem. Eng. Data 47, 313–315. https://doi.org/10.1021/je0102199.

Takeya, S., Shimada, W., Kamata, Y., Ebinuma, T., Uchida, T., Nagao, J., Narita, H., 2001. In situ x-ray diffraction measurements of the self-preservation effect of CH_4 hydrate. J. Phys. Chem. 105, 9756–9759. https://doi.org/10.1021/jp011435r.

Wang, W.X., Bray, C.L., Adams, D.J., Cooper, A.I., 2008. Methane storage in dry water gas hydrates. J. Am. Chem. Soc. 130, 11608–11609. https://doi.org/10.1021/ja8048173.

Wang, W.X., Zeng, P.Y., Long, X.Y., Huang, J.R., Liu, Y., Tan, B.E., Sun, L.Y., 2014. Methane storage in tea clathrates. Chem. Commun. 50, 1244–1246. https://doi.org/10.1039/c3cc47619g.

Wu, Q., Yu, Y., Zhang, B.Y., Gao, X., Zhang, Q., 2019. Effect of temperature on safety and stability of gas hydrate during coal mine gas storage and transportation. Saf. Sci. 118, 264–272. https://doi.org/10.1016/j.ssci.2019.04.034.

Xiao, P., Yang, X.M., Li, W.Z., Cui, J.L., Sun, C.Y., Chen, G.J., Chen, J.L., 2019. Improving methane hydrate formation in highly water-saturated fixed bed with diesel oil as gas channel. Chem. Eng. J. 368, 299–309. https://doi.org/10.1016/j.cej.2019.02.139.

Xiao, P., Yang, X.M., Sun, C.Y., Cui, J.L., Li, N., Chen, G.J., 2018. Enhancing methane hydrate formation in bulk water using vertical recipro cating impact. Chemcial Engineering Journal 336, 649–658. https://doi.org/10.1016/j.cej.2017.12.020.

Xie, Y., Zheng, T., Zhong, J.R., Zhu, Y.J., Wang, Y.F., Zhang, Y., Li, R., Yuan, Q., Sun, C.Y., Chen, G.J., 2020. Experimental research on self-preservation effect of methane hydrate in porous sediments. Appl. Energy 268, 115008. https://doi.org/10.1016/j.apenergy.2020.115008.

Xie, Y., Zhu, Y.J., Zheng, T., Yuan, Q., Sun, C.Y., Yang, L.Y., Chen, G.J., 2021. Replacement in CH_4-CO_2 hydrate below freezing point based on abnormal self-preservation differences of CH_4 hydrate. Chem. Eng. J. 403, 126283. https://doi.org/10.1016/j.cej.2020.126283.

Xu, S.R., Fan, S.S., Fang, S.T., Lang, X.M., Wang, Y.H., Chen, J., 2016. Pectin as an extraordinary natural kinetic hydrate inhibitor. Sci. Rep. 6, 23220. https://doi.org/10.1038/srep23220.

Yan, K.L., Sun, C.Y., Chen, J., Chen, L.T., Shen, D.J., Liu, B., Jia, M.L., Niu, M., Lv, Y.N., Li, N., Song, Z.Y., Niu, S.S., Chen, G.J., 2014. Flow characteristics and rheological properties of natural gas hydrate slurry in the presence of anti-agglomerant in a flow loop apparatus. Chem. Eng. Sci. 106, 99–108. https://doi.org/10.1016/j.ces.2013.11.015.

Yang, M.J., Zheng, J.N., Gao, Y., Ma, Z.Q., Lv, X., Song, Y.C., 2019. Dissociation characteristics of methane hydrates in South China Sea sediments by depressurization. Appl. Energy 243, 266–273. https://doi.org/10.1016/j.apenergy.2019.03.160.

Zeng, Y.S., Chen, J., Yu, X.Y., Wang, T., Deng, B., Zeng, F.H., Li, J.Y., 2020. Suppression of methane hydrate dissociation from SDS-dry solution hydrate formation system by a covering liquid method. Fuel 277, 118222. https://doi.org/10.1016/j.fuel.2020.118222.

Zhang, G.C., Rogers, R.E., 2008. Ultra-stability of gas hydrates at 1 atm and 268.2K. Chem. Eng. Sci. 63, 2066–2074. https://doi.org/10.1016/j.ces.2008.01.008.

Zheng, J.J., Loganathan, N.K., Zhao, J.Z., Linga, P., 2019. Clathrate hydrate formation of CO_2/CH_4 mixture at room temperature: application to direct transport of CO_2-containing natural gas. Appl. Energy 249, 190–203. https://doi.org/10.1016/j.apenergy.2019.04.118.

Zhong, J.R., Zeng, X.Y., Zhou, F.H., Ran, Q.D., Sun, C.Y., Zhong, R.Q., Yang, L.Y., Chen, G.J., Koh, C.A., 2016. Self-preservation and structural transition of gas hydrates during dissociation below the ice point: an in situ study using Raman spectroscopy. Sci. Rep. 6, 38855. https://doi.org/10.1038/srep38855.